Supporting Information

A High-density Energetic Ammonium Salt via a Polynitropyrazolate Counteranion

Miao Li,[a] Yubei Zhang,[a] Yaqun Dong,[b] Jing Liu,[a] Yuji Liu,[a] Wei Huang,[a] Chuan Xiao,*[c] Guangbin Cheng,[a] Yongxing Tang*[a]

[a]School of Chemistry and Chemical Engineering, Nanjing University of Science and Technology, Nanjing 210094 (China).

[b]Luzhou Northern Chemical Industry Co., Ltd, Sichuan 646000, China.

[c]China Northern Industries Group Co., Ltd (NORINCO GROUP), Beijing 100089, China.

Table of Contents

1. General methods

^{1}H and ^{13}C NMR spectra were recorded on a Bruker AVANCE III 300 MHz nuclear magnetic resonance spectrometer. DMSO-d_6 was used as solvent and locking solvent. The working frequencies for ^{1}H and ^{13}C are 300 MHz and 75 MHz, respectively. Chemical shifts were reported relative to tetramethylsilane as internal standard. Decomposition temperatures (onset) were obtained on a TA Instruments DSC25 differential scanning calorimeter at a heating rate of 5 °C min^{-1}. Infrared spectra (IR) were recorded on a PerkinElmer Spectrum BX FT-IR instrument equipped with an ATR unit at 25 °C. Elemental analyses of C/H/N were performed on a Vario EL III Analyzer. Impact and friction sensitivities were measured with a BAM fallhammer and friction tester. The densities were measured by AccuPyc II 1345 gas pycnometer (Micromeritics). X-ray intensity data were collected on a Bruker D8 VENTURE PHOTON II system equipped with an Incoatecius 3.0 Microfocus sealed tube. The structures were solved and refined using Bruker SHELXTL Software Package. The data were refined against F^2. All non-hydrogen atoms were refined anisotropically. Hydrogen atoms were fixed to their parent atoms using a riding model and refined isotropically.

2. Computational methods

The gas-phase heats of formation were calculated by using the isodesmic reactions (Scheme S1). The enthalpy of reaction was obtained by combining the MP2/6-311++G** energy difference for reactions, the scaled zero-point energies (ZPE), values of thermal correction (HT), and other thermal factors. The solid-state heats of formation for **2** anion was estimated by subtracting gas-phase enthalpies with the corresponding enthalpy of sublimation (ΔH_{sub}). In equation 1, T represents either the melting point or decomposition temperature when no melting occurs prior to decomposition.

ΔH_{sub}=188/J mol^{-1} K^{-1}×T (1)

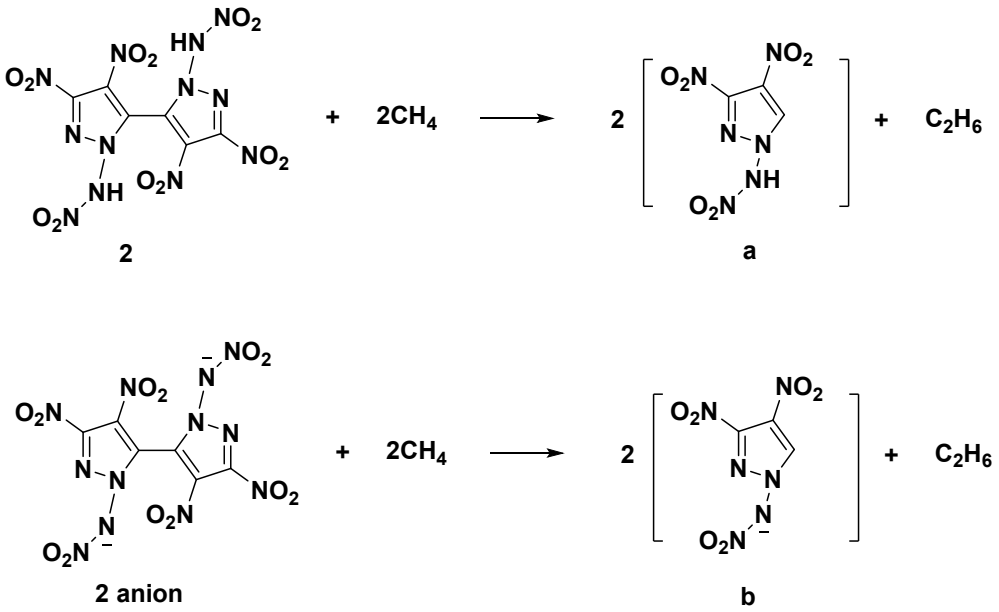

Scheme S1. Isodesmic reactions for **2** and **2** anion.

Table S1. Calculated zero-point energy (ZPE), values of the correction (Hr), total energy (E_0) and heats of formation (HOF)

Species	ZPE	H_r	E_0	Corrected E_0	HOF (kJ mol^{-1})
2	0.168456	0.195175	-1785.000564	-1784.81213	884.8400573
a	0.094081	0.10754	-893.073118	-892.96934	350.6617043
b	0.081064	0.094034	-892.583409	-892.49262	70.91969078
2 anion	0.142009	0.167877	-1783.945157	-1783.78296	183.4976094
CH_4	0.044793	0.048605	-40.3796224	-40.33281	-74.6
C_2H_6	0.074599	0.079027	-79.5716306	-79.49559	-84

[a] Data obtained from G2.

Table S2. Calculated solid state heat of formation (HOF)

Compound	ΔH_L (kJ/mol)	ΔH_f^{Cation} (kJ/mol)	ΔH_f^{Anion} (kJ/mol)	ΔH_f^{298} (KJ/mol)
2	/	/	/	814.2
2a	1162.216623	626.4	183.5	274.1
2b	1062.109639	671.1	183.5	463.6

Table S3. Cartesian coordinates (in Å) of the DFT-optimized structure of **2**.

Number	Symbol	Coordinates (Å)		
		X	Y	Z
1	C	4.089	24.517	9.017
2	C	6.021	25.038	9.908
3	C	4.685	24.801	10.227
4	C	2.724	24.139	8.648
5	C	2.007	22.98	8.83
6	C	0.825	23.165	8.119
7	N	5.077	24.586	8.096
8	N	6.265	24.916	8.622
9	N	0.775	24.36	7.548
10	N	1.932	24.924	7.877
11	N	5.001	24.439	6.706
12	N	4.82	23.145	6.412
13	N	7.127	25.475	10.763
14	N	4.037	24.709	11.507
15	N	2.512	21.812	9.49
16	N	-0.287	22.285	7.906
17	N	2.25	26.144	7.294
18	N	2.154	27.102	8.195
19	O	4.879	22.881	5.194
20	O	8.248	25.153	10.446
21	O	4.735	24.465	12.488
22	O	2.189	20.722	9.044
23	O	-0.454	21.371	8.693
24	O	1.907	26.91	9.375
25	O	4.597	22.264	7.264
26	O	6.838	26.174	11.725
27	O	2.82	24.85	11.54
28	O	3.249	21.991	10.463
29	O	-0.997	22.495	6.926
30	O	2.355	28.264	7.738
31	H	2.51157	26.27559	6.33783
32	H	5.07068	25.18117	6.03943

Table S4. Cartesian coordinates (in Å) of the DFT-optimized structure of **2a**.

Number	Symbol	Coordinates (Å)		
		X	Y	Z
1	C	4.089	24.517	9.017
2	C	6.021	25.038	9.908
3	C	4.685	24.801	10.227
4	C	2.724	24.139	8.648
5	C	2.007	22.98	8.83
6	C	0.825	23.165	8.119
7	N	5.077	24.586	8.096
8	N	6.265	24.916	8.622
9	N	0.775	24.36	7.548
10	N	1.932	24.924	7.877
11	N	5.001	24.439	6.706
12	N	4.82	23.145	6.412
13	N	7.127	25.475	10.763
14	N	4.037	24.709	11.507
15	N	2.512	21.812	9.49
16	N	-0.287	22.285	7.906
17	N	2.25	26.144	7.294
18	N	2.154	27.102	8.195
19	O	4.879	22.881	5.194
20	O	8.248	25.153	10.446
21	O	4.735	24.465	12.488
22	O	2.189	20.722	9.044
23	O	-0.454	21.371	8.693
24	O	1.907	26.91	9.375
25	O	4.597	22.264	7.264
26	O	6.838	26.174	11.725
27	O	2.82	24.85	11.54
28	O	3.249	21.991	10.463
29	O	-0.997	22.495	6.926
30	O	2.355	28.264	7.738
31	N	1.189	27.391	12.024
32	H	1.666	26.895	11.524
33	H	1.039	26.988	12.76
34	H	1.604	28.118	12.184
35	H	0.449	27.562	11.638
36	N	3.387	27.524	5.286
37	H	4.123	27.202	5.569
38	H	2.971	27.896	5.927
39	H	3.543	28.097	4.677
40	H	2.909	26.893	4.964

Table S5. Cartesian coordinates (in Å) of the DFT-optimized structure of **2b**.

Number	Symbol	Coordinates (Å)		
		X	Y	Z
1	C	1.10201	3.4749	4.3539
2	C	3.09481	4.0123	5.27294
3	C	1.78974	4.18954	5.44982
4	C	-0.20875	3.26238	4.19803
5	C	-1.00163	3.07883	2.96418
6	C	-2.27654	3.26833	3.2876
7	N	2.21272	3.05013	3.46896
8	N	3.42473	3.20696	4.21204
9	N	-2.49954	3.51003	4.61981
10	N	-1.20572	3.75434	5.17846
11	N	2.10117	2.59952	2.19915
12	N	3.23153	2.23783	1.49301
13	N	3.96458	4.54415	6.02354
14	N	1.23922	4.84667	6.38142
15	N	-0.55107	2.79466	1.81571
16	N	-3.21108	3.229	2.43446
17	N	-0.94187	4.32605	6.37488
18	N	-1.97992	4.73782	7.18733
19	O	3.12296	1.79923	0.25702
20	O	5.24418	4.333	5.8002
21	O	0.99428	6.13023	6.22547
22	O	-0.211	3.75748	0.98555
23	O	-4.45624	3.42432	2.81298
24	O	-1.72309	5.2943	8.3519
25	O	4.41726	2.33177	2.05611
26	O	3.58909	5.30815	7.02712
27	O	0.91191	4.24617	7.50575
28	O	-0.42279	1.53643	1.45204
29	O	-2.93736	2.9928	1.16909
30	O	-3.22593	4.57371	6.79697
31	N	0.12608	-1.07359	-1.23186
32	C	-0.2972	-1.82538	-2.15836
33	N	0.53712	-2.56252	-2.82957
34	N	-1.53299	-1.8593	-2.43119
35	N	0.08508	-3.36537	-3.81901
36	H	-0.54779	-0.47821	-0.68972
37	H	1.15102	-1.04545	-1.00557
38	H	1.55718	-2.53451	-2.60436
39	H	-1.88405	-2.48282	-3.19962
40	H	-2.20686	-1.26392	-1.88906
41	H	0.73971	-3.94375	-4.34566

42	H	-0.91057	-3.39271	-4.03883
43	N	1.87592	7.72731	14.47222
44	C	1.45264	6.97552	13.54572
45	N	2.28696	6.23838	12.87451
46	N	0.21685	6.94159	13.27289
47	N	1.83492	5.43552	11.88507
48	H	1.20205	8.32269	15.01436
49	H	2.90086	7.75544	14.69851
50	H	3.30702	6.26638	13.09972
51	H	-0.13421	6.31807	12.50446
52	H	-0.45702	7.53697	13.81502
53	H	2.48955	4.85715	11.35842
54	H	0.83927	5.40819	11.66525

3. Interaction of different energetic ammonium salts with water molecules

The task was set to DMol3-Geometry Optimization to optimize the molecular conformation. The functional used was GGA-BLYP, with a basis set of DNP-3.5 and All electron core treatment. The convergence criteria were set as follows: energy convergence at 2.0×10^{-5} Ha, force convergence at 0.004 Ha/Å, Max Iteration at 500, and Maximum Step Size at 0.3 Å. It is crucial to ensure that the final results converge. After the optimization is complete, the interaction energy calculation was performed by setting the task to DMol3-Energy using the GGA-BLYP functional. The ammonium salt and water molecules were designated as Set1 and Set2, respectively, with the BSSE correction enabled. After the calculation is complete, the interaction energy can be obtained by reviewing the results. The non-bonding interaction distances can be measured by selecting the Distance option in the Measure-Change toolbar.

Interaction energy calculation:

The interaction energy (E_{int}), indicating the intensity of interaction between the components in the system, is derived according to the following equation:

$$E_{int} = E_{total} - \Sigma E_{component} + E_{bsse} \quad (2)$$

where E_{total} and $E_{componen}$ represent the total energy of the system, and the energy of each component in the system, respectively. E_{bass} represents BSSE correction energy. More negative E_{int} indicates a stronger interaction in the system.

Table S6. The interaction energy between **2a**, ammonium dinitramide (ADN) and water molecule

Compound	E_{total} (kcal/mol)	E_{H2O} (kcal/mol)	$E_{component}$ (kcal/mol)	E_{BSSE} (kcal/mol)	E_{int} (kcal/mol)
2a•H_2O	-1241729.23	-47974.00	-1120105.70	0.34073793	-4.71
ADN•H_2O	-375709.21	-47973.81	-327715.24	0.55095378	-19.62

4. Experimental section

Caution! All new compounds in this work are potentially energetic materials that could explode under certain conditions, such as impact, friction and high temperature. Although there were no explosions during this work, appropriate safety precautions must be taken (safety glasses, face shields, earplugs, and gloves).

Synthesis of 2,2'-dinitroamino-4,4',5,5'-tetranitro-2*H*,2'*H*-3,3'-bipyrazole (2)

To a mixture of sulfuric acid (98%, 2.0 mL) and nitric acid (100%, 1.0 mL) was added compound **1** (0.34 g, 1.0 mmol) at -15 °C. The reaction mixture was stirred for 4 hours at this temperature. Then the white precipitate was collected and dried by air.

2: White solid (0.36 g, yield: 83 %). T_d (onset): 103 °C. ^{1}H NMR (300 MHz, CD_3CN): δ = 7.54 (s, 2H) ppm; ^{13}C NMR (76 MHz, CD_3CN) δ = 148.4, 129.1, 126.2 ppm; Elemental analysis for $C_6H_2N_{12}O_{12}$ (434.15): Calcd C 16.60, H 0.46, N 38.72; found: C 16.49, H 0.64, N 38.45.

General procedures for the preparation of energetic salts (2a-2b)

Compound **2** (0.87 g, 2 mmol) was suspended in water and 2.2 equivalents of bases (aqueous ammonia, water solution of aminoguanidine bicarbonate) were dropped at room temperature. The reaction was stirred 1h the formed precipitate was collected by filtration. The crude product was purified by recrystallization from water solution.

2a: Yellow solid. (0.65 g, yield: 78 %). T_d (onset): 180 °C. ^{1}H NMR (300 MHz, MeOD): δ = 7.30 (s, 8H) ppm; ^{13}C NMR (76 MHz, MeOD): δ = 146.8, 126.7, 126.6 ppm; IR (KBr): ṽ 3289, 2974, 2894, 1731, 1627, 1604, 1519, 1472, 1406, 1312, 1170, 1138, 987, 831, 794, 747, 713, 534 cm^{-1}. Elemental analysis for $C_6H_8N_{14}O_{12}$ (468.22): Calcd C 15.39, H 1.72, N 41.88. Found: C 15.55, H 2.00, N 41.73.

2b: Yellow solid. (0.89 g, yield: 76 %). T_d (onset): 200 °C. ^{1}H NMR (300 MHz, MeOD): δ = 7.08 (s,

2H), 4.64 (s, 2H) ppm; ^{13}C NMR (76 MHz, MeOD): δ = 160.5, 146.6, 126.5, 126.4 ppm; IR (KBr): $\tilde{\nu}$ 3605, 3252, 3049, 2851, 1608, 1537, 1400, 1353, 1259, 1080, 1043, 991, 925, 897, 840, 803, 746, 732, 553 cm^{-1}. Elemental analysis for $C_8H_{14}N_{20}O_{12}$ (582.33): Calcd C 16.50, H 2.42, N 48.11. Found: C 16.72, H 2.60, N 47.98.

Table S7. Densities and detonation velocities of 2a and representative ammonium salts of nitroamine compounds.

Compounds	Molecular structures	Density (298 K)	Detonation velocity (m s^{-1})	Ref
2a	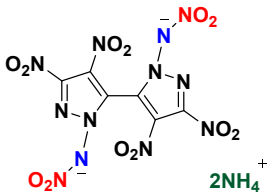	**1.88**	**9134**	**This work**
A	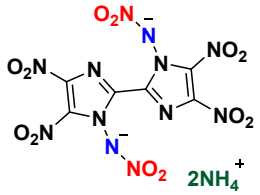	**1.78**	**8745**	**[1]**
B	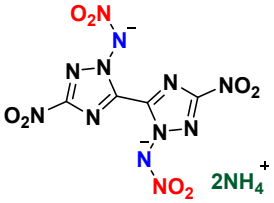	**1.77**	**8865**	**[2]**
C	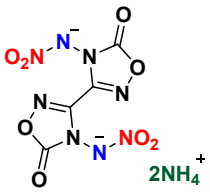	**1.827**	**8796**	**[3]**
D	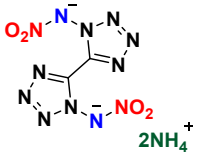	**1.795**	**9438**	**[4]**
E	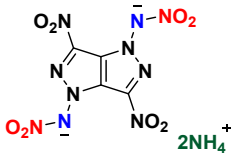	**1.81**	**8999**	**[5]**

F	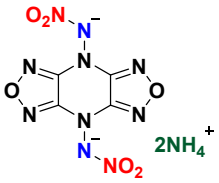	**1.757**	**8809**	**[6]**
G	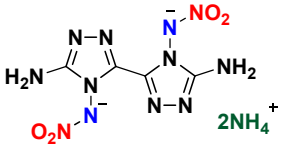	**1.67**	**8625**	**[7]**
H	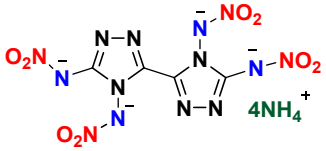	**1.75**	**8883**	**[8]**
I	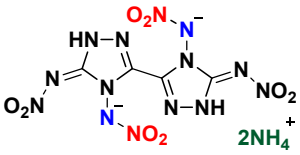	**1.82**	**9194**	**[8]**
J	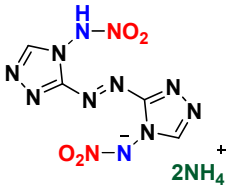	**1.729**	**8430**	**[9]**
K	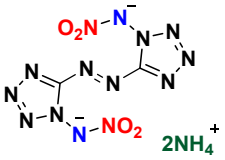	**1.753**	**9396**	**[4]**
L	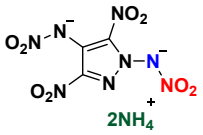	**1.80**	**8982**	**[10]**
M	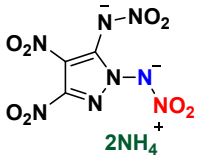	**1.74**	**8816**	**[10]**
N	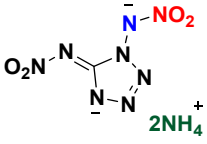	**1.689**	**9067**	**[11]**
O	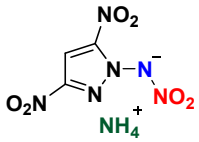	**1.77**	**8773**	**[10]**

P	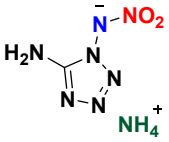	**1.757**	**9111**	**[12]**

5. Crystal structure data

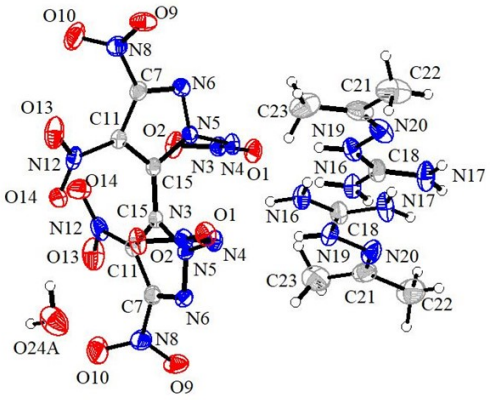

Figure S1. single-crystal X-ray structure of **2b**·**0**.65H_2O

Crystals of **2b**·0.65H_2O suitable for X-ray diffraction were obtained by slow evaporation of its saturated solutions in acetone at room temperature. Notably, during the crystal growth process, aminoguanidinium reacted with the acetone solvent. Although the crystal quality was suboptimal, the fundamental structure of **2b** was unequivocally confirmed.

Table S8. Crystal data and structure refinement for **2a**·0.67H_2O.

compound	**2a**·0.67H_2O
Empirical formula	$C_{18}H_{28}N_{42}O_{38}$
Formula weight	1440.82
Temperature [K]	130(2)
Crystal system	Monoclinic
Space group	*C*2/c (15)
a [Å]	8.6521(11)
b [Å]	28.997(2)
c [Å]	21.0931(19)
α [°]	90
β [°]	103.523(4)
γ [°]	90
V [Å^3]	5203.0(9)
Z	4
ρ_{calcd} [Mg·m^{-3}]	1.839

μ/mm^{-1}	1.573
F(000)	2936
Crystal size	0.15 × 0.1 × 0.1 mm^3
Theta range for data collection	6.10 to 136.80 (0.83 Å)
index ranges	-8 ≤ h ≤ 10, -34 ≤ k ≤ 34, -25 ≤ l ≤ 25
reflections collected	17903
independent reflections (R_{int})	4711 [R_{int} = 0.0512]
data / restraints / parameters	4711/1342/491
GOF on F^2	1.145
Final R indices [I>=2σ (I)]	R_1 = 0.0655, wR_2 = 0.1722
R indices [all data]	R_1 = 0.0682, wR_2 = 0.1736
CCDC number	2418270

Table S9. Fractional Atomic Coordinates (×10^4) and Equivalent Isotropic Displacement Parameters (Å2×10^3) for **2a**·0.67H_2O. Ueq is defined as 1/3 of the trace of the orthogonalized Uij tensor.

	x	y	z	Ueq
C1	0.6662(4)	0.84551(12)	0.43478(17)	0.0183(7)
C2	0.9086(4)	0.86346(12)	0.47777(17)	0.0180(7)
C3	0.7611(4)	0.85531(12)	0.49315(17)	0.0171(7)
C4	0.5005(4)	0.83248(12)	0.41701(17)	0.0185(7)
C5	0.4216(4)	0.79251(12)	0.42579(18)	0.0194(7)
C6	0.2697(4)	0.79886(12)	0.39149(18)	0.0192(7)
C7	0.3588(4)	0.52416(12)	0.11384(17)	0.0176(7)
C8	0.4748(4)	0.50705(12)	0.16303(17)	0.0171(7)
C9	0.4568(4)	0.53211(11)	0.21685(17)	0.0154(7)
N1S	0.7606(4)	0.84787(11)	0.39037(15)	0.0215(6)
N2	0.9092(4)	0.85927(11)	0.41576(15)	0.0227(7)
N3	0.2516(4)	0.84008(10)	0.36395(15)	0.0195(6)
N4	0.3924(3)	0.85952(9)	0.37985(14)	0.0159(6)
N5	0.7220(4)	0.84282(13)	0.32338(16)	0.0307(8)
N6	0.6948(4)	0.79817(13)	0.30919(16)	0.0313(8)
N7	1.0548(3)	0.87854(10)	0.51898(14)	0.0180(6)
N8	0.7137(3)	0.85211(10)	0.55488(14)	0.0174(6)
N9	0.4941(4)	0.75222(11)	0.45762(19)	0.0313(8)
N10	0.1366(4)	0.76853(11)	0.38124(17)	0.0264(7)
N11	0.4166(4)	0.90160(10)	0.35173(15)	0.0229(7)
N12	0.4249(3)	0.93464(10)	0.39515(14)	0.0173(6)

N13	0.3357(3)	0.56124(10)	0.19641(14)	0.0173(6)
N14	0.2728(4)	0.55669(10)	0.13437(15)	0.0191(6)
N15	0.3165(4)	0.50926(11)	0.04754(15)	0.0222(7)
N16	0.5986(3)	0.47402(10)	0.16122(14)	0.0178(6)
N17	0.2827(4)	0.59685(10)	0.23208(15)	0.0223(7)
N18	0.2003(4)	0.57842(11)	0.27360(15)	0.0211(7)
O1	0.6754(4)	0.78909(14)	0.25046(15)	0.0504(10)
O2	1.1776(3)	0.86742(10)	0.50370(14)	0.0265(6)
O3	0.8154(3)	0.84370(9)	0.60218(12)	0.0259(6)
O4	0.4472(4)	0.71463(10)	0.4361(2)	0.0564(10)
O5	0.1342(4)	0.73700(11)	0.41918(16)	0.0394(8)
O6	0.4217(4)	0.92802(10)	0.45205(14)	0.0376(8)
O7	0.6873(3)	0.76779(10)	0.35028(14)	0.0320(7)
O8	1.0421(3)	0.90265(9)	0.56539(13)	0.0259(6)
O9	0.5737(3)	0.85699(10)	0.55645(13)	0.0265(6)
O10	0.6002(4)	0.75839(12)	0.50451(17)	0.0443(9)
O11	0.0335(3)	0.77578(10)	0.33399(16)	0.0346(7)
O12	0.4383(3)	0.97473(8)	0.37313(13)	0.0237(6)
O13	0.2250(4)	0.53302(10)	0.01063(13)	0.0321(7)
O14	0.6644(3)	0.47405(10)	0.11495(13)	0.0271(6)
O15	0.1782(3)	0.53655(9)	0.27904(13)	0.0251(6)
O16	0.3735(4)	0.47285(10)	0.03338(14)	0.0334(7)
O17	0.6339(3)	0.44867(8)	0.20842(13)	0.0233(6)
O18	0.1463(3)	0.60747(9)	0.30820(13)	0.0280(6)
N1_1	0.3956(4)	0.94460(10)	0.57978(14)	0.0196(6)
H1A_1	0.440(3)	0.9275(8)	0.5557(12)	0.029
H1B_1	0.394(4)	0.9307(9)	0.6153(8)	0.029
H1C_1	0.447(3)	0.9697(6)	0.5875(14)	0.029
H1D_1	0.3018(15)	0.9505(10)	0.5612(13)	0.029
O1_2	0.6051(4)	0.81230(11)	0.70608(17)	0.0425(8)
H1A_2	0.651(7)	0.8371(12)	0.699(2)	0.064
H1B_2	0.561(7)	0.8031(18)	0.6689(12)	0.064
N1_5	-0.008(6)	0.86038(19)	0.252(2)	0.022(3)
H1A_5	-0.042330	0.849811	0.214809	0.034
H1B_5	0.033526	0.886669	0.249671	0.034
H1C_5	-0.083795	0.862814	0.272911	0.034
H1D_5	0.060506	0.841833	0.272602	0.034
N1_8	0.4497(10)	0.6998(3)	0.2663(4)	0.0301(19)

H1A_8	0.381798	0.679299	0.270490	0.045
H1B_8	0.504402	0.706230	0.302900	0.045
H1C_8	0.509359	0.689777	0.241426	0.045
H1D_8	0.402558	0.724044	0.249792	0.045
N1_7	0.3402(8)	0.6845(2)	0.3182(3)	0.0272(16)
H1A_7	0.343763	0.655693	0.310822	0.041
H1B_7	0.245071	0.693211	0.313913	0.041
H1C_7	0.387665	0.690112	0.356455	0.041
H1D_7	0.385544	0.699123	0.291581	0.041
N1_6	0.505(6)	0.9492(2)	0.2549(18)	0.019(3)
H1A_6	0.596081	0.938097	0.268547	0.029
H1B_6	0.470585	0.962032	0.285804	0.029
H1C_6	0.509878	0.968949	0.225511	0.029
H1D_6	0.442804	0.927452	0.239347	0.029

Table S10. Bond lengths [Å] and angles [°] for **2a**·0.67H_2O

Atom	Lengths/Å	Atom	Angles/°
C1–N1S	1.352(5)	N1S–C1–C3	105.8(3)
C1–C3	1.379(5)	N1S–C1–C4	121.5(3)
C1–C4	1.463(5)	C3–C1–C4	132.6(3)
C2–N2	1.314(5)	N2–C2–C3	112.7(3)
C2–C3	1.394(5)	N2–C2–N7	117.3(3)
C2–N7	1.464(5)	C3–C2–N7	129.8(3)
C3–N8	1.438(5)	C1–C3–C2	104.4(3)
C4–N4	1.355(5)	C1–C3–N8	125.0(3)
C4–C5	1.375(5)	C2–C3–N8	130.3(3)
C5–C6	1.392(5)	N4–C4–C5	105.0(3)
C5–N9	1.434(5)	N4–C4–C1	122.6(3)
C6–N3	1.326(5)	C5–C4–C1	132.1(3)
C6–N10	1.433(5)	C4–C5–C6	105.3(3)
C7–N14	1.322(5)	C4–C5–N9	124.4(3)
C7–C8	1.396(5)	C6–C5–N9	129.9(3)
C7–N15	1.446(5)	N3–C6–C5	111.8(3)
C8–C9	1.380(5)	N3–C6–N10	117.4(3)
C8–N16	1.443(5)	C5–C6–N10	130.8(3)
C9–N13	1.354(5)	N14–C7–C8	112.4(3)
C9–C9$^{\#1}$	1.460(7)	N14–C7–N15	118.1(3)
N1S–N2	1.341(4)	C8–C7–N15	129.3(3)

N1S–N5	1.399(5)	C9–C8–C7	104.5(3)
N3–N4	1.329(4)	C9–C8–N16	124.5(3)
N4–N11	1.389(4)	C7–C8–N16	130.7(3)
N5–N6	1.340(5)	N13–C9–C8	105.3(3)
N6–O7	1.246(4)	N13–C9–C9	122.4(3)
N6–O1	1.248(4)	C8–C9–C9	132.3(3)
N7–O2	1.210(4)	N2–N1S–C1	113.1(3)
N7–O8	1.224(4)	N2–N1S–N5	117.6(3)
N8–O9	1.226(4)	C1–N1S–N5	129.2(3)
N8–O3	1.228(4)	C2–N2–N1S	104.0(3)
N9–O4	1.221(5)	C6–N3–N4	104.0(3)
N9–O10	1.234(5)	N3–N4–C4	113.9(3)
N10–O5	1.218(5)	N3–N4–N11	117.9(3)
N10–O11	1.229(5)	C4–N4–N11	127.8(3)
N11–N12	1.318(4)	N6–N5–N1S	109.1(3)
N12–O6	1.221(4)	O7–N6–O1	121.8(4)
N12–O12	1.265(4)	O7–N6–N5	123.9(3)
N13–N14	1.329(4)	O1–N6–N5	114.3(3)
N13–N17	1.403(4)	O2–N7–O8	125.2(3)
N15–O13	1.217(4)	O2–N7–C2	117.9(3)
N15–O16	1.225(4)	O8–N7–C2	116.8(3)
N16–O14	1.216(4)	O9–N8–O3	124.5(3)
N16–O17	1.230(4)	O9–N8–C3	117.6(3)
N17–N18	1.338(4)	O3–N8–C3	117.9(3)
N18–O15	1.238(4)	O4–N9–O10	125.1(4)
N18–O18	1.259(4)	O4–N9–C5	117.8(4)

Table S11. Anisotropic displacement parameters ($Å^2$ x 10^3) for **2a**·0.67H_2O. The anisotropic displacement factor exponent takes the form: $-2\pi^2$ [$h^2a^{*2}U^{11}$+ ... + 2 h k a* b* U^{12}].

	U^{11}	U^{22}	U^{33}	U^{23}	U^{13}	U^{12}
C1	0.0179(15)	0.0174(15)	0.0203(16)	0.0046(13)	0.0050(13)	−0.0040(13)
C2	0.0156(16)	0.0181(15)	0.0207(16)	−0.0006(13)	0.0046(13)	−0.0030(13)
C3	0.0159(15)	0.0161(15)	0.0198(16)	0.0022(13)	0.0046(13)	−0.0002(12)
C4	0.0171(16)	0.0182(15)	0.0209(16)	0.0018(13)	0.0049(13)	−0.0003(13)
C5	0.0166(16)	0.0149(15)	0.0291(17)	0.0047(13)	0.0103(13)	0.0020(13)
C6	0.0178(16)	0.0150(15)	0.0270(17)	−0.0042(13)	0.0101(14)	−0.0004(13)
C7	0.0186(16)	0.0136(15)	0.0217(17)	0.0010(13)	0.0066(13)	−0.0020(13)
C8	0.0165(16)	0.0138(15)	0.0220(16)	−0.0003(13)	0.0063(13)	−0.0031(13)

C9	0.0182(16)	0.0100(14)	0.0193(16)	0.0007(12)	0.0071(13)	−0.0002(12)
N1S	0.0178(14)	0.0287(15)	0.0180(14)	0.0027(12)	0.0031(11)	−0.0103(12)
N2	0.0176(15)	0.0273(15)	0.0233(15)	−0.0009(12)	0.0041(12)	−0.0070(12)
N3	0.0183(14)	0.0183(14)	0.0221(14)	−0.0050(11)	0.0038(12)	0.0004(11)
N4	0.0194(14)	0.0093(12)	0.0181(13)	0.0010(10)	0.0014(11)	−0.0023(11)
N5	0.0298(17)	0.0428(19)	0.0196(15)	0.0015(14)	0.0052(13)	−0.0173(15)
N6	0.0303(18)	0.044(2)	0.0206(17)	−0.0026(15)	0.0080(14)	−0.0197(16)
N7	0.0167(15)	0.0140(13)	0.0235(15)	−0.0001(12)	0.0039(12)	−0.0025(11)
N8	0.0169(15)	0.0148(13)	0.0206(15)	0.0004(11)	0.0036(12)	−0.0008(11)
N9	0.0234(17)	0.0207(17)	0.055(2)	0.0190(15)	0.0218(16)	0.0079(13)
N10	0.0188(16)	0.0220(16)	0.0414(19)	−0.0080(14)	0.0133(15)	−0.0035(13)
N11	0.0398(17)	0.0109(13)	0.0172(14)	0.0013(11)	0.0029(13)	−0.0017(12)
N12	0.0173(14)	0.0148(14)	0.0209(15)	−0.0018(11)	0.0060(12)	−0.0001(11)
N13	0.0192(14)	0.0128(13)	0.0209(14)	0.0010(11)	0.0065(12)	0.0019(11)
N14	0.0194(14)	0.0171(14)	0.0221(15)	0.0019(11)	0.0073(12)	−0.0007(11)
N15	0.0199(15)	0.0208(15)	0.0258(16)	−0.0035(13)	0.0035(13)	−0.0023(12)
N16	0.0181(14)	0.0134(13)	0.0226(15)	−0.0030(12)	0.0059(12)	−0.0016(11)
N17	0.0331(17)	0.0146(14)	0.0232(15)	0.0032(12)	0.0153(13)	0.0065(12)
N18	0.0190(15)	0.0241(16)	0.0207(15)	0.0066(12)	0.0051(12)	0.0071(12)
O1	0.057(2)	0.074(2)	0.0221(16)	−0.0146(16)	0.0130(15)	−0.0367(19)
O2	0.0140(13)	0.0320(15)	0.0349(15)	−0.0072(12)	0.0081(11)	−0.0032(11)
O3	0.0252(14)	0.0316(15)	0.0199(13)	0.0031(11)	0.0010(11)	0.0041(11)
O4	0.051(2)	0.0154(15)	0.111(3)	0.0106(17)	0.036(2)	0.0047(14)
O5	0.0377(18)	0.0374(17)	0.0474(18)	0.0018(14)	0.0192(14)	−0.0169(14)
O6	0.067(2)	0.0281(15)	0.0234(15)	−0.0047(12)	0.0223(14)	−0.0058(14)
O7	0.0313(16)	0.0365(16)	0.0298(15)	−0.0037(12)	0.0101(12)	−0.0122(12)
O8	0.0218(14)	0.0280(14)	0.0273(14)	−0.0080(11)	0.0026(11)	−0.0030(11)
O9	0.0167(13)	0.0335(15)	0.0319(15)	0.0026(12)	0.0110(11)	0.0021(11)
O10	0.0232(16)	0.054(2)	0.058(2)	0.0356(17)	0.0135(15)	0.0152(14)
O11	0.0185(14)	0.0264(15)	0.0551(19)	−0.0061(13)	−0.0030(13)	−0.0031(11)
O12	0.0302(15)	0.0111(12)	0.0300(14)	0.0006(10)	0.0060(11)	−0.0004(10)
O13	0.0382(17)	0.0317(15)	0.0235(14)	0.0009(12)	−0.0018(12)	0.0053(13)
O14	0.0257(14)	0.0319(15)	0.0261(14)	−0.0036(11)	0.0113(12)	0.0036(11)
O15	0.0217(14)	0.0221(13)	0.0330(15)	0.0078(11)	0.0089(11)	−0.0004(11)
O16	0.0356(16)	0.0288(15)	0.0334(16)	−0.0150(12)	−0.0004(13)	0.0041(12)
O17	0.0236(13)	0.0161(12)	0.0308(15)	0.0024(11)	0.0065(11)	0.0036(10)
O18	0.0370(16)	0.0269(14)	0.0231(14)	0.0054(11)	0.0138(12)	0.0155(12)
N1_1	0.0219(16)	0.0209(15)	0.0178(15)	−0.0016(12)	0.0078(12)	−0.0014(12)

O1_2	0.043(2)	0.0300(17)	0.058(2)	−0.0157(15)	0.0181(17)	−0.0122(14)
N1_5	0.020(7)	0.017(2)	0.028(6)	0.002(6)	0.000(4)	0.000(6)
N1_8	0.031(4)	0.023(4)	0.035(4)	0.002(3)	0.001(3)	−0.005(3)
N1_7	0.036(3)	0.021(3)	0.022(3)	−0.005(2)	0.000(2)	−0.007(2)
N1_6	0.028(4)	0.020(2)	0.012(8)	0.001(5)	0.008(5)	0.004(6)

Table S12. Torsion angles [°] for **2a**·0.67H_2O.

Atom	Angles/°	Atom	Angles/°
N1S–C1–C3–C2	0.7(4)	N2–N1S–N5–N6	110.5(4)
C4–C1–C3–C2	177.7(4)	C1–N1S–N5–N6	−73.8(5)
N1S–C1–C3–N8	−173.3(3)	N1S–N5–N6–O7	7.9(5)
C4–C1–C3–N8	3.7(6)	N1S–N5–N6–O1	−172.9(3)
N2–C2–C3–C1	−0.1(4)	N2–C2–N7–O2	−31.8(5)
N7–C2–C3–C1	175.3(3)	C3–C2–N7–O2	152.9(4)
N2–C2–C3–N8	173.4(3)	N2–C2–N7–O8	146.2(3)
N7–C2–C3–N8	−11.1(6)	C3–C2–N7–O8	−29.1(5)
N1S–C1–C4–N4	−67.8(5)	C1–C3–N8–O9	−26.8(5)
C3–C1–C4–N4	115.6(4)	C2–C3–N8–O9	160.9(4)
N1S–C1–C4–C5	104.9(5)	C1–C3–N8–O3	151.7(3)
C3–C1–C4–C5	−71.7(6)	C2–C3–N8–O3	−20.7(5)
N4–C4–C5–C6	0.9(4)	C4–C5–N9–O4	−142.4(4)
C1–C4–C5–C6	−172.8(4)	C6–C5–N9–O4	29.2(6)
N4–C4–C5–N9	174.2(3)	C4–C5–N9–O10	37.0(5)
C1–C4–C5–N9	0.6(7)	C6–C5–N9–O10	−151.4(4)
C4–C5–C6–N3	−1.2(4)	N3–C6–N10–O5	−159.5(3)
N9–C5–C6–N3	−174.0(4)	C5–C6–N10–O5	21.6(6)
C4–C5–C6–N10	177.8(4)	N3–C6–N10–O11	21.6(5)
N9–C5–C6–N10	5.0(7)	C5–C6–N10–O11	−157.3(4)
N14–C7–C8–C9	−0.9(4)	N3–N4–N11–N12	108.1(3)
N15–C7–C8–C9	−176.4(3)	C4–N4–N11–N12	−79.8(4)
N14–C7–C8–N16	−175.6(3)	N4–N11–N12–O6	4.3(5)
N15–C7–C8–N16	8.9(6)	N4–N11–N12–O12	−176.4(3)
C7–C8–C9–N13	0.0(4)	C8–C9–N13–N14	0.9(4)
N16–C8–C9–N13	175.2(3)	$C9^{\#1}$–C9–N13–N14	179.1(3)
C7–C8–C9–$C9^{\#1}$	−178.0(4)	C8–C9–N13–N17	−173.3(3)
N16–C8–C9–$C9^{\#1}$	−2.8(6)	$C9^{\#1}$–C9–N13–N17	4.9(5)
C3–C1–N1S–N2	−1.1(4)	C8–C7–N14–N13	1.4(4)
C4–C1–N1S–N2	−178.5(3)	N15–C7–N14–N13	177.4(3)

C3–C1–N1S–N5	−176.9(4)	C9–N13–N14–C7	−1.4(4)
C4–C1–N1S–N5	5.6(6)	N17–N13–N14–C7	173.3(3)
C3–C2–N2–N1S	−0.5(4)	N14–C7–N15–O13	14.1(5)
N7–C2–N2–N1S	−176.6(3)	C8–C7–N15–O13	−170.6(4)
C1–N1S–N2–C2	1.0(4)	N14–C7–N15–O16	−164.3(3)
N5–N1S–N2–C2	177.4(3)	C8–C7–N15–O16	11.0(5)
C5–C6–N3–N4	1.0(4)	C9–C8–N16–O14	−136.8(4)
N10–C6–N3–N4	−178.1(3)	C7–C8–N16–O14	36.9(5)
C6–N3–N4–C4	−0.4(4)	C9–C8–N16–O17	40.6(5)
C6–N3–N4–N11	172.8(3)	C7–C8–N16–O17	−145.6(4)
C5–C4–N4–N3	−0.3(4)	N14–N13–N17–N18	109.5(3)
C1–C4–N4–N3	174.1(3)	C9–N13–N17–N18	−76.6(4)
C5–C4–N4–N11	−172.7(3)	N13–N17–N18–O15	0.9(5)
C1–C4–N4–N11	1.7(6)	N13–N17–N18–O18	−179.8(3)

6. NMR spectra

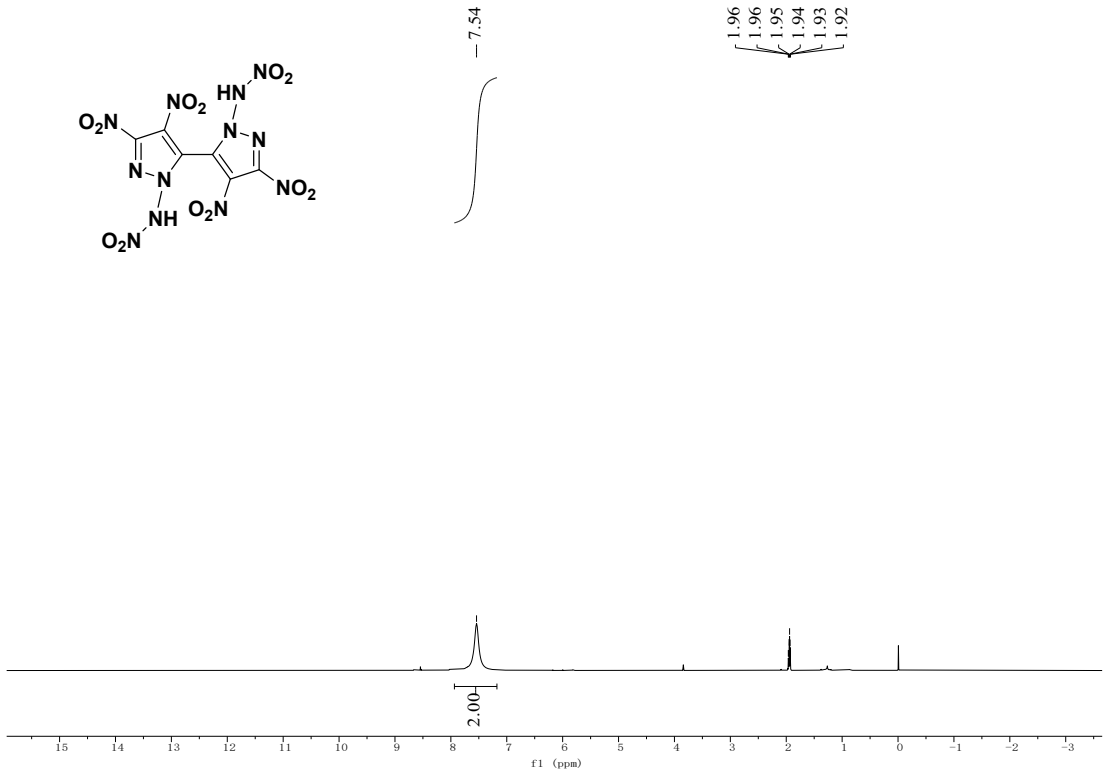

Figure S2. ^{1}H NMR spectrum of **2**

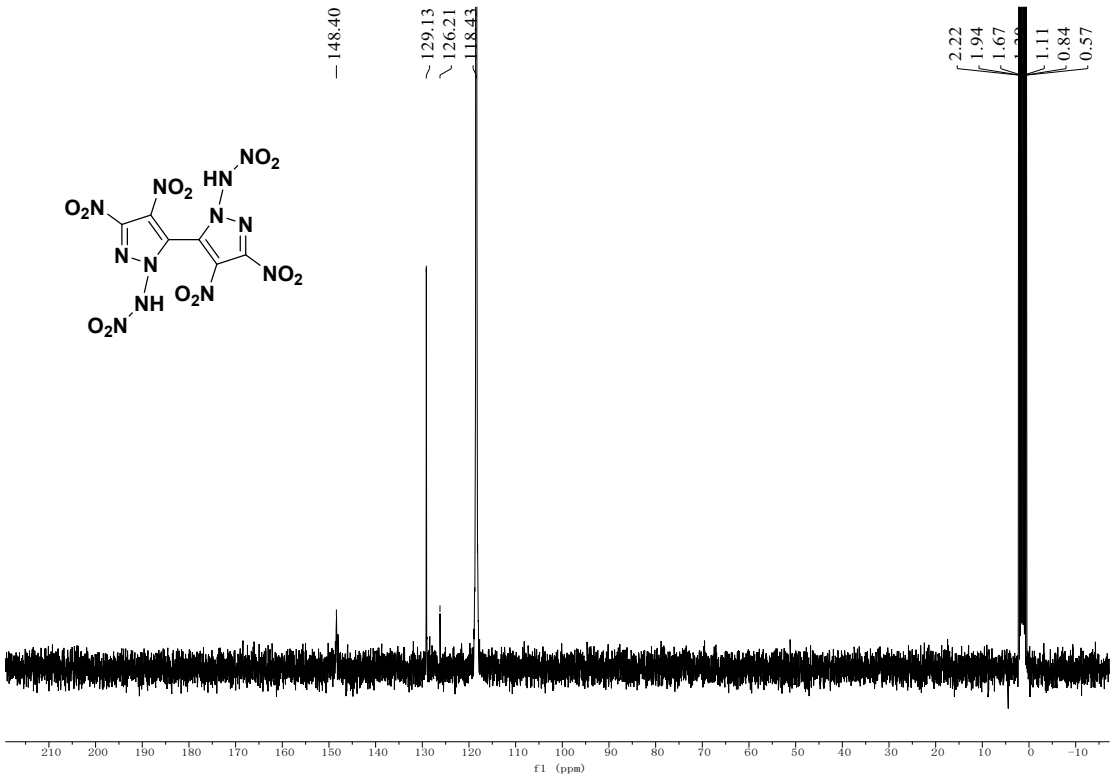

Figure S3. ^{13}C NMR spectrum of **2**

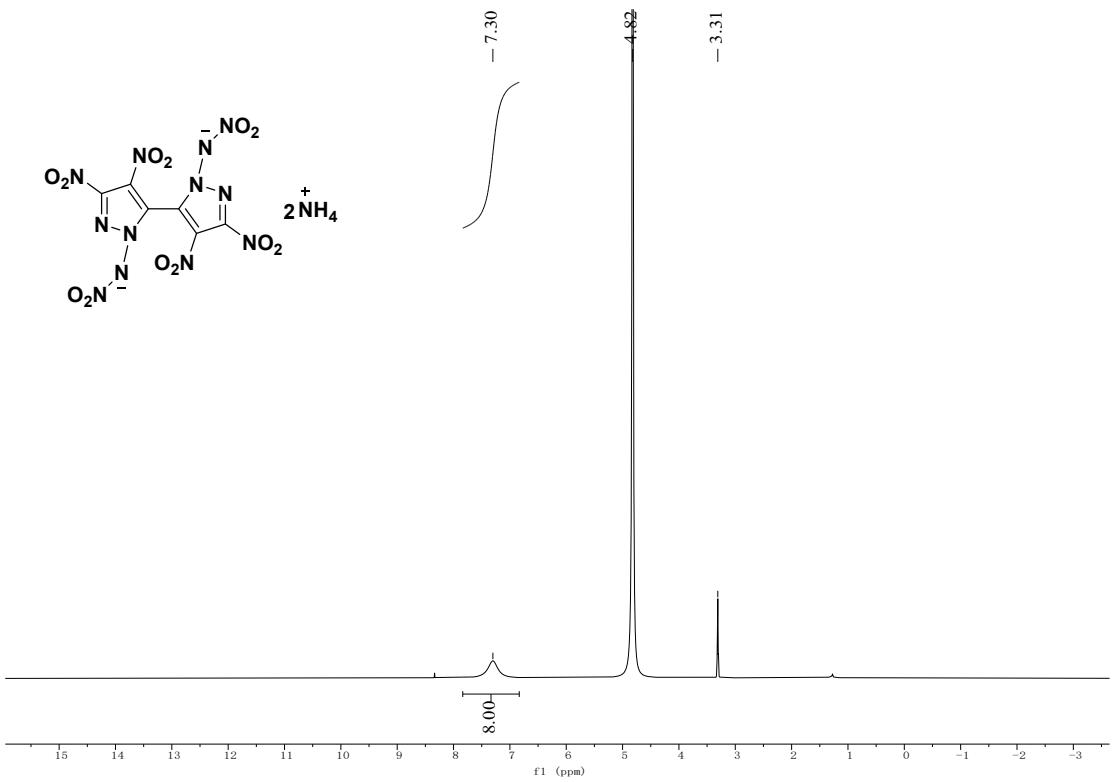

Figure S4. ^{1}H NMR spectrum of **2a**

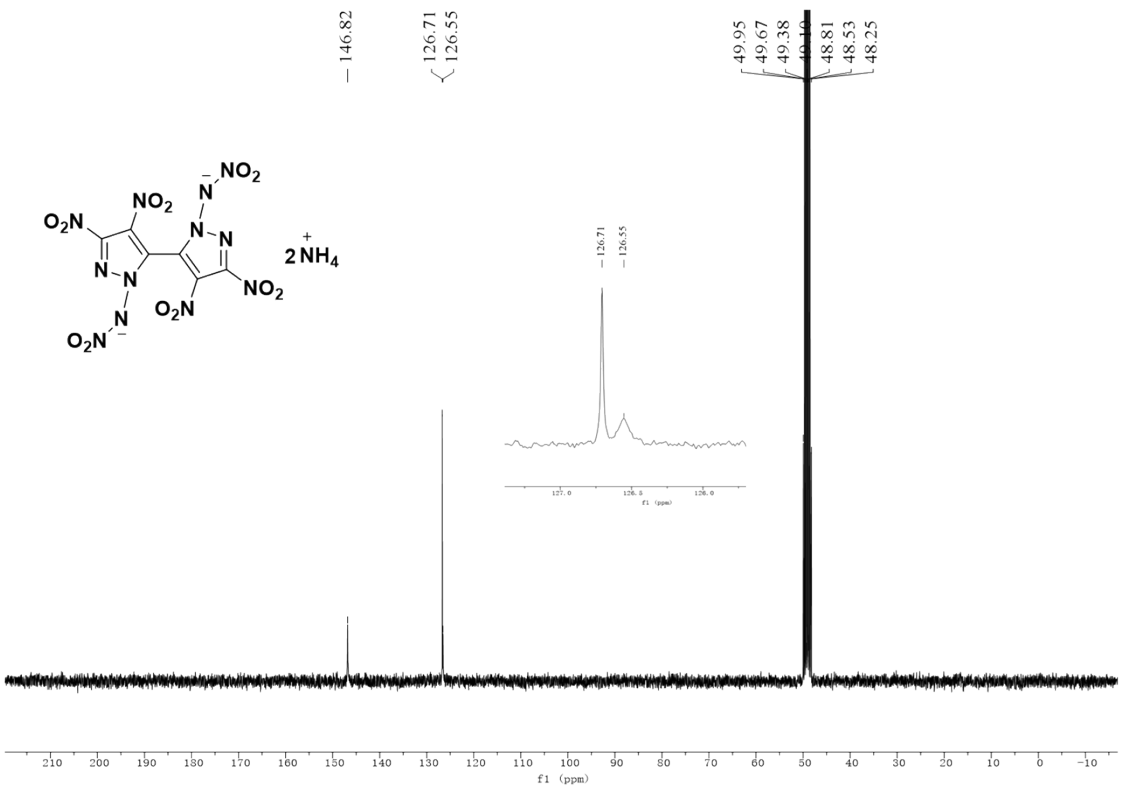

Figure S5. ^{13}C NMR spectrum of **2a**

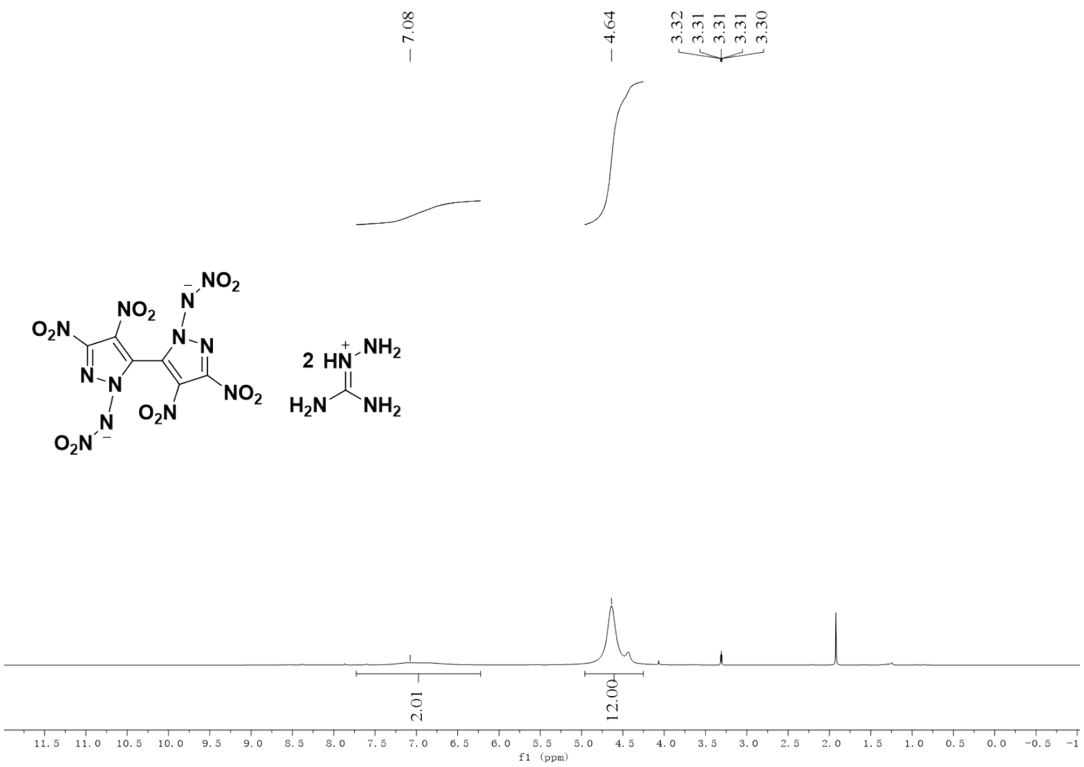

Figure S6. ^{1}H NMR spectrum of **2b**

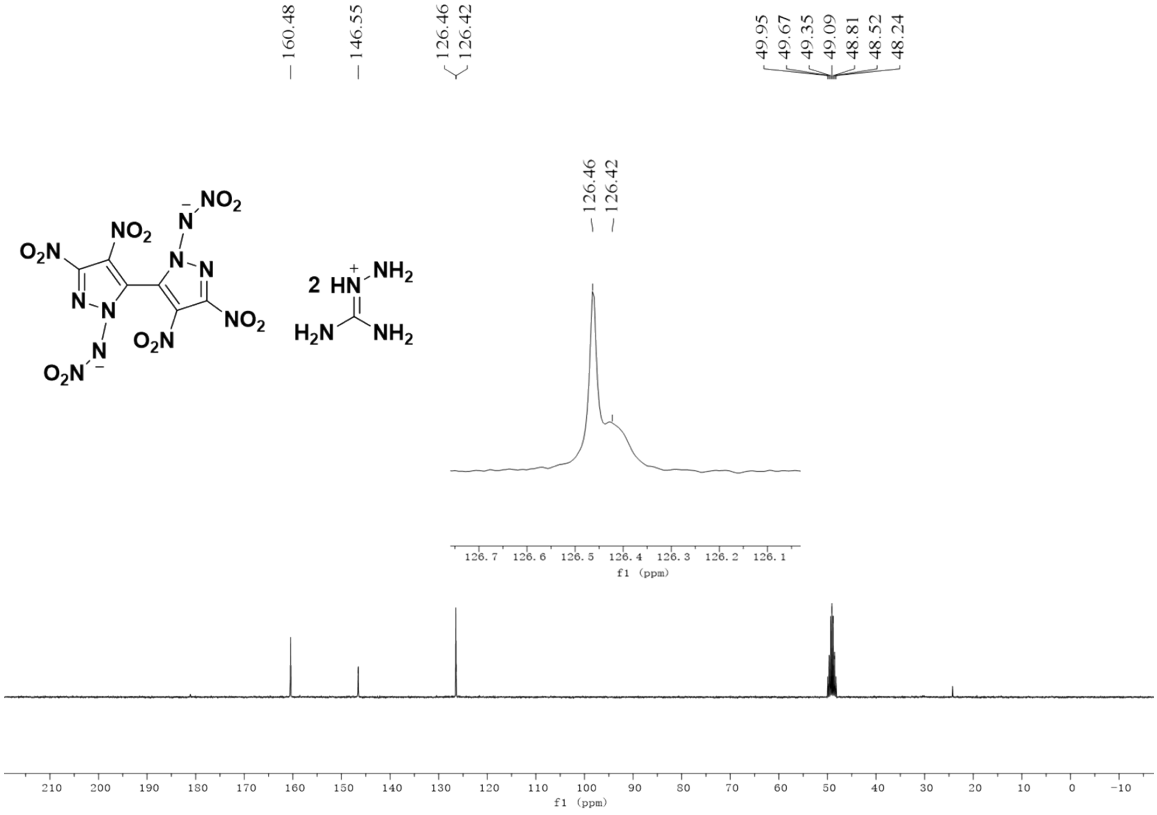

Figure S7. ^{13}C NMR spectrum of **2b**

7. DSC plots

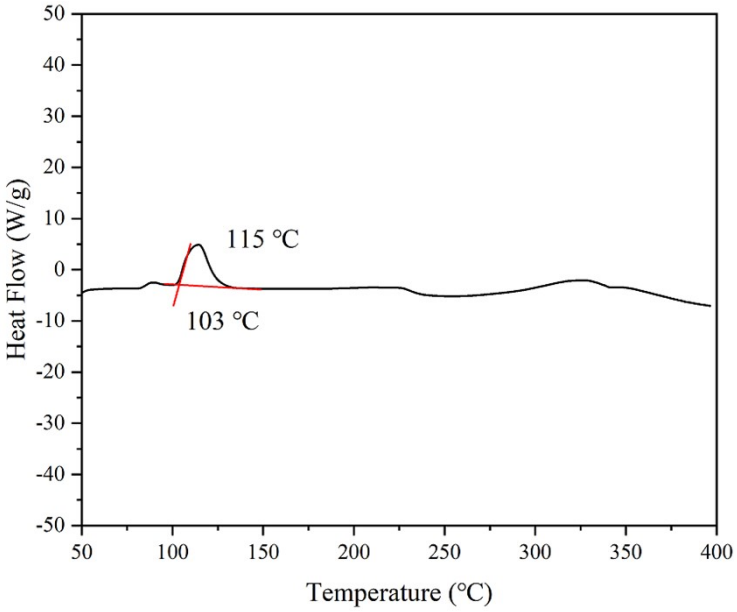

Figure S8. DSC plot of **2**

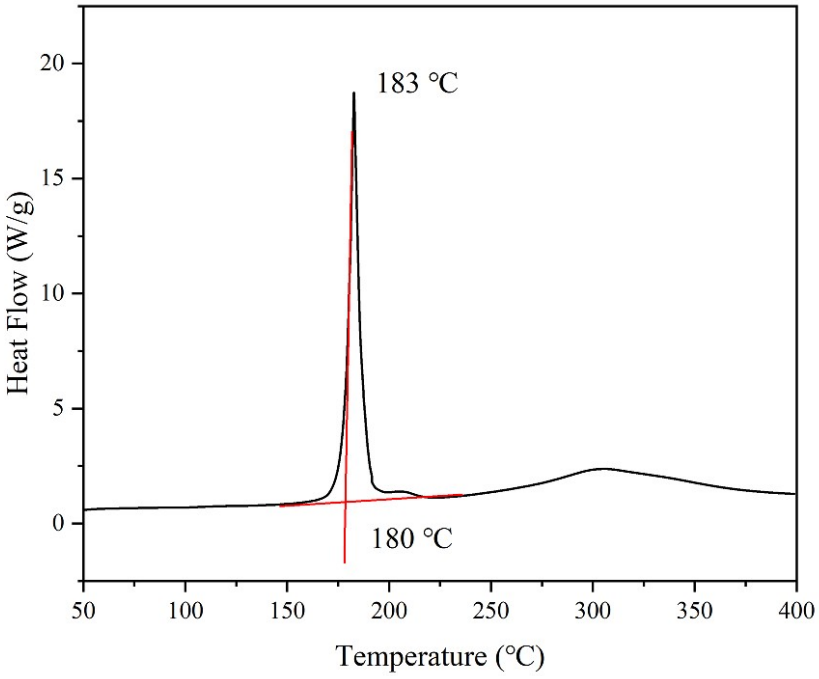

Figure S9. DSC plot of **2a**

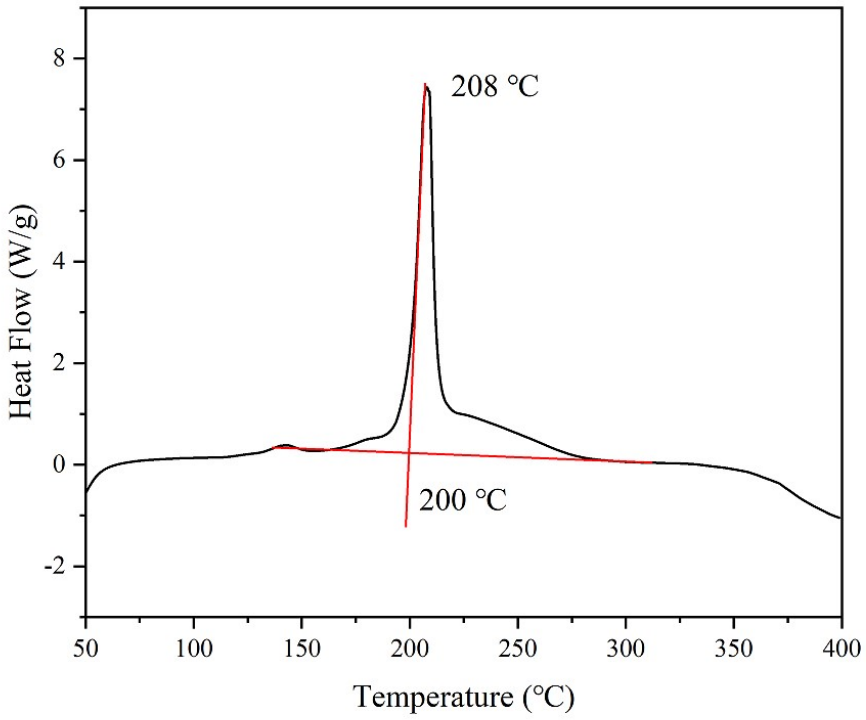

Figure S10. DSC plot of **2b**

REFERENCES

(1) Yin, P.; He, C.; Shreeve, J. M. Fully C/N-polynitro-functionalized 2,2'-biimidazole derivatives as nitrogen-and oxygen-rich energetic salts. *Chem. Eur. J.* **2016**, *22*(6), 2108–2113.

(2) Yin, P.; Shreeve, J. M. From *N*-nitro to *N*-nitroamino: preparation of high-performance energetic materials by introducing nitrogen-containing ions. *Angew. Chem. Int. Ed.* **2015**, *54*(48), 14513–14517.

(3) Cai, J.; Zhang, J.; Xiong, J.; Li, R.; Fei, T.; Lai, Q.; Yin, P.; Pang, S. The intramolecular integration of carbonyl and *N*-nitroamino groups to effectively balance the energy and sensitivity of *N*-nitroamino-functionalized bisazoles. *Chem. Eng. J.* **2023**, *467*, 143527.

(4) Fischer, D.; Klapötke, T. M.; Stierstorfer, J.; Szimhardt, N. 1,1′-Nitramino-5,5′-bitetrazoles. *Chem. Eur. J.* **2016**, *22*(14), 4966–4970

(5) Yin, P.; Zhang, J.; Mitchell, L. A.; Parrish, D. A.; Shreeve, J. M. 3,6-Dinitropyrazolo[4,3-*c*]pyrazole-based multipurpose energetic materials through versatile *N*-functionalization strategies. *Angew. Chem. Int. Ed.* **2016**, *55*(41), 12895–12897.

(6) Li, W.; Tian, J.; Qi, X.; Wang, K.; Jin, Y.; Wang, B.; Zhang, Q. Synthesis of 4,8-dinitraminodifurazano[3, 4-b,e]pyrazine derived nitrogen-rich salts as potential energetic materials. *ChemistrySelect* **2018**, *3*(2), 849–854.

(7) Klapötke, T. M.; Leroux, M.; Schmid, P. C.; Stierstorfer, J.; Energetic materials based on 5,5′-diamino-4,4′-dinitramino-3,3′-bi-1,2,4-triazole. *Chem. Asian J.* **2015**, *11*(6), 844–851.

(8) Lang, Q.; Sun, Q.; Wang, Q.; Lin, Q.; Lu, M. Embellishing bis-1,2,4-triazole with four nitroamino groups: advanced high-energy-density materials with remarkable performance and good stability. *J. Mater. Chem. A* **2020**, *8*(23), 11752–11760.

(9) Yount, J.; Zeller, M.; Byrd, E. F. C.; Piercey, D. G. 4,4’-Dinitrimino-5,5’-diamino-3,3’-azo-bis-1,2,4-triazole: a high-performing zwitterionic energetic material. *Inorg. Chem.* **2021**, *60*(21), 16204–16212.

(10) Yin, P.; Parrish, D. A.; Shreeve, J. M. Energetic multifunctionalized nitraminopyrazoles and their ionic derivatives: ternary hydrogen-bond induced high energy density materials. *J. Am. Chem. Soc.* **2015**, *137*(14), 4778–4786.

(11) Fischer, D.; Klapötke, T. M.; Stierstorfer, J. 1,5-Di(nitramino)tetrazole: high sensitivity and superior explosive performance. *Angew. Chem. Int. Ed.* **2015**, *54*(35), 10299–10302.

(12) Klapötke, T. M.; Martin, F. A.; Stierstorfer, J.; N-Bound primary nitramines based on 1,5-diaminotetrazole. *Chem. Eur. J.* **2012**, *18*(5), 1487–1501.